

Null device-independent prepare-and-prepare bipartite dimension test with a single joint measurement

Josep Batle^{1,2,*}, Tomasz Białeccki^{3,4}, and Adam Bednorz^{3†}

¹ *Departament de Física and Institut d'Aplicacions Computacionals de Codi Comunitari (IAC3), Campus UIB, E-07122 Palma de Mallorca, Balearic Islands, Spain*

² *CRISP – Centre de Recerca Independent de sa Pobla, 07420, sa Pobla, Balearic Islands, Spain*

³ *Faculty of Physics, University of Warsaw, ul. Pasteura 5, PL02-093 Warsaw, Poland and*

⁴ *University of Lodz, Faculty of Physics and Applied Informatics, ul. Pomorska 149/13, PL90-236 Łódź, Poland*

We propose a device-independent dimensionality test with bipartite measurements and input from two separate parties, based on a null witness. The dimension is determined from the rank of the matrix of measurements for pairs of states prepared by the parties. We have applied the test to various IBM Quantum devices. The results demonstrate extreme precision of the test, which is able to detect disagreements with the qubit (two-level) space of bipartite measurement even in the presence of technical imperfections. The deviations beyond 6 standard deviations have no simple origin and need urgent explanations to unblock progress in quantum computing.

I. INTRODUCTION

Quantum bipartite systems have nonclassical properties, they violate local realism [1–5] and are useful in quantum computation. The very, if not the most, important part of quantum operations is measurement. The measurement often completes the dynamics and reflects the knowledge about the quantum state. A single measurement does not reveal the full quantum state and gives a random outcome, is invasive, and triggers decoherence and collapse. To find out the full state, one has to repeat the same experiment many times to gain decent statistics and to make a tomography, a set of incompatible measurements, to fully recover the corresponding density matrix. On the other hand, it is important to assess the dimension of the states and measurements in question (quantum or classical) for the error correction and mitigation tools to work, assuming restricted Hilbert spaces [6–8].

Although the number of outcomes is always quite arbitrary, the measurement cannot increase the dimension of the input states. There are methods that determine the dimension of the space of a single state. They require a dimension witness, usually in the prepare-and-measure (PM) scenario, i.e. one prepares a state from a certain set and a measurement also from another set. The matrix of probabilities obtained is constrained by the dimension. The early witnesses based on inequality [9, 10] are outperformed by the null witnesses, where the equality to zero is a signature of the dimension [11–13]. Null witnesses turn out to be extremely precise in the detection of an extra space in real devices [14, 15].

The situation becomes more complicated if the measured state itself comes from two parties, especially when they are independent of each other. A way of dimension testing is to check the Schmidt number of a bipar-

tite state [16, 17], i.e. the locally irreducible dimension of the state. It allows replacing the inefficient PM scenario by the measure-and-measure (MM) protocol, when only measurements are chosen on each party, or even one makes just a single measurement with many outcomes. Such tests turned out to be extremely precise when quantifying the entanglement space [18].

Here we propose yet another perspective, namely, to test the dimension of two parties in a joint measurement, i.e. prepare-and-prepare (PP) scenario. It is similar to reversing the MM setup, with a few caveats. Each party chooses to prepare its state independently in one of the initial states. The measurement channel does not depend on the states but its outcome does, resulting in a probability matrix, whose rank corresponds to the bipartite dimension. The actual witness is the determinant of the probability matrix [19], equal to zero for sufficiently large sets of prepared states, with finite statistical error. It is critical to assume independence between parties, as otherwise the additional correlation affects the conclusion.

We have demonstrated the validity of the test in the two-level case on IBM Quantum with the measurement of a single qubit, between the two single-qubit parties. Most tests have been positive. However, there are several strong failures. They cannot be explained by simple technical imperfections, as the test is robust to local noise and the quantum operation differs only by a phase, and is not synchronized with other qubits.

The paper is organized as follows. We start from the witness construction, then we show the implementation of the test on IBM Quantum. We present the results and discuss them, paying attention to their reliability and calibration errors. Detailed explanations are given in the Appendices.

II. THE WITNESS

Suppose we have a composite (tensor) system of A and B and the initially prepared state $\rho_{ij} = A_i \otimes B_j$, where

* jbv276@uib.es, batlequantum@gmail.com

† Adam.Bednorz@fuw.edu.pl

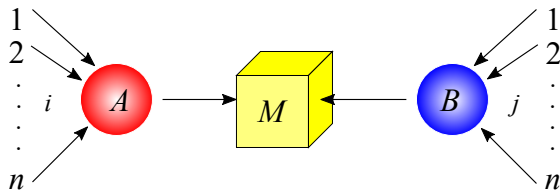


FIG. 1. Two parties A and B perform either one of n independent preparations indexed by i and j , respectively. The joint measurement takes the prepared states as inputs.

A_i and B_j are local states (Hermitian $A_i^\dagger = A_i$, positive $A_i \geq 0$, and subjected to normalization via $\text{Tr}A_i$, and similarly for B_j), in the respective subspaces [20], $i, j = 1 \dots n$. To shorten the notation, we shall drop the tensor sign whenever unambiguous, i.e. $AB \equiv A \otimes B$. The joint measurement in the combined space is $0 \leq \mathcal{M} \leq 1$, which occurs with the probability

$$p_{ij} = \text{Tr} \mathcal{M} A_i B_j. \quad (1)$$

Now p is a $n \times n$ matrix of probabilities p_{ij} for all combinations of states prepared independently by A and B . The rank of the matrix p depends on the dimension d of the input spaces, loosely related to the old definition of the Schmidt number [16, 17]. We shall assume as Schmidt number just the minimal dimension of the A and B spaces.

Our witness is the $n \times n$ determinant $W_n = \det p$ which is equal 0 if the Schmidt number satisfies $d < n$ (classical case) $d^2 < n$ (quantum complex) or $d(d+1)/2 < n$ (quantum real) because the size of p exceeds the maximal rank of the set of allowed matrices A_i or B_j , which span the available linear space. If the dimension of the linear space of observables is smaller than the size of the matrix then some observable must be a linear combination of the rest. By linearity of the matrix (1) as a function of the observables, the same applies to its corresponding column or row, and the determinant must vanish. The real symmetric matrix $d \times d$ is represented by $d(d+1)/2$ independent real numbers. A complex Hermitian matrix has additionally $d(d-1)/2$ real independent numbers, representing imaginary antisymmetric matrices. The test is device-independent, that is, we make no assumption about the actual realization of preparations or measurements. Simply, the test does not rely on the mathematical model. However, we assume independence of A and B as otherwise we cannot write the concomitant tensor product.

In particular, the witness is zero in the case $d = 2$ for $n > 2$ in the classical case, $n > 3$ in the quantum real case, and $n > 4$ in the full complex case. If $W_5 \neq 0$ then we have a classical system of dimension 5 or a quantum one of dimension 3 (real or complex). It can be easily tested on available quantum computers.

In the non-zero cases, W is still bounded. The classical maximum is reached whenever $d = n$, by the Hadamard determinant, i.e. $A_i = |i\rangle\langle i| = B_i$ with $\mathcal{M} = M_{ij}|ij\rangle\langle ij|$.

n	1	2	3	4	5	6	7	8	9
$\max W_n$	1	1	2	3	5	9	32	56	144

TABLE I. The classical maximum of W_n equivalent to a maximal determinant of the $n \times n$ matrix with entries of 0 or 1.

The values of W are given in Table I and the corresponding matrices M are shown in Table II.

III. ERROR ANALYSIS

To determine the value of the witness W_n , we collect data from N repetitions of each measurement combination. The uncertainty in determining W_n is analogous to the prepare-measure scheme in Ref.[13] for finite statistics and assuming $\langle W_n \rangle = 0$. From Laplace expansion

$$\delta W = \sum_{kj} \delta p_{kj} (\mathcal{A})_{jk}, \quad (2)$$

where $\mathcal{A} = \text{Adj } p$ is the adjugate matrix (matrix of minors of p , without given row and column, and then transposed). The variance $N \Delta W_n^2$, is

$$\sum_{kj} \mathcal{A}_{jk}^2 p_{kj} (1 - p_{kj}), \quad (3)$$

with the adjugate matrix calculated directly, since $p\mathcal{A} = \det p$ cannot be inverted when $\det p = 0$. One should also avoid the situation of $\mathcal{A} = 0$, i.e. when the rank is already smaller, as the error becomes not reliable, and one has to consider second-order minors.

IV. DEMONSTRATION ON IBM QUANTUM

We have demonstrated the feasibility of the above test on IBM Quantum devices. A microwave pulse tuned to the interlevel drive frequency allows one to apply the parametrically controlled gates. The native single qubit gate is the $\pi/2$ rotation

$$S = \sqrt{X} = X_+ = (\sigma_0 - i\sigma_1)/\sqrt{2}, \quad (4)$$

in the $|0\rangle, |1\rangle$ basis. The rotation for a given angle θ is realized with the native gate S and two gates Z_θ

$$S_\theta = Z_\theta^\dagger S Z_\theta, \quad Z_\theta = \sigma_0 \cos \theta/2 - i\sigma_3 \sin \theta/2, \quad (5)$$

with shorthand notation $Z = Z_\pi$, $Z_\pm = Z_{\pm\pi/2}$. In addition, there is a native two-qubit *CNOT* gate on most of IBM quantum devices, operating as

$$|00\rangle\langle 00| + |01\rangle\langle 01| + |11\rangle\langle 10| + |10\rangle\langle 11|, \quad (6)$$

where for $|ab\rangle$ the control qubit states are a (depicted as \bullet) and the target qubit state is b (depicted as \oplus in Fig.

$$(1), \begin{pmatrix} 1 & 0 \\ 0 & 1 \end{pmatrix}, \begin{pmatrix} 1 & 0 & 1 \\ 1 & 1 & 0 \\ 0 & 1 & 1 \end{pmatrix}, \begin{pmatrix} 0 & 1 & 1 & 1 \\ 1 & 1 & 0 & 1 \\ 1 & 0 & 1 & 1 \\ 1 & 1 & 1 & 0 \end{pmatrix}, \begin{pmatrix} 1 & 0 & 0 & 1 & 1 \\ 0 & 1 & 0 & 1 & 1 \\ 0 & 0 & 1 & 1 & 1 \\ 1 & 1 & 1 & 0 & 1 \\ 1 & 1 & 1 & 1 & 0 \end{pmatrix}, \begin{pmatrix} 1 & 0 & 0 & 1 & 1 & 0 \\ 0 & 1 & 0 & 0 & 1 & 1 \\ 1 & 0 & 1 & 0 & 0 & 1 \\ 1 & 1 & 0 & 1 & 0 & 0 \\ 0 & 1 & 1 & 0 & 1 & 0 \\ 0 & 0 & 1 & 1 & 0 & 1 \end{pmatrix},$$

$$\begin{pmatrix} 1 & 0 & 1 & 0 & 1 & 0 & 1 \\ 0 & 1 & 1 & 0 & 0 & 1 & 1 \\ 1 & 1 & 0 & 0 & 1 & 1 & 0 \\ 0 & 0 & 0 & 1 & 1 & 1 & 1 \\ 1 & 0 & 1 & 1 & 0 & 1 & 0 \\ 1 & 1 & 0 & 1 & 0 & 0 & 1 \\ 0 & 1 & 1 & 1 & 1 & 0 & 0 \end{pmatrix}, \begin{pmatrix} 1 & 0 & 1 & 0 & 0 & 1 & 1 & 0 \\ 1 & 1 & 0 & 1 & 0 & 0 & 1 & 1 \\ 1 & 1 & 1 & 0 & 1 & 0 & 0 & 1 \\ 0 & 1 & 1 & 1 & 0 & 1 & 0 & 0 \\ 0 & 0 & 1 & 1 & 1 & 0 & 1 & 0 \\ 1 & 1 & 0 & 1 & 1 & 1 & 0 & 1 \\ 1 & 0 & 0 & 1 & 1 & 1 & 0 & 1 \\ 0 & 1 & 0 & 0 & 1 & 1 & 1 & 0 \\ 0 & 0 & 1 & 0 & 0 & 1 & 1 & 1 \end{pmatrix}, \begin{pmatrix} 0 & 1 & 1 & 1 & 1 & 1 & 1 & 0 & 0 \\ 1 & 0 & 1 & 1 & 1 & 1 & 0 & 1 & 0 \\ 1 & 1 & 0 & 1 & 1 & 0 & 1 & 1 & 0 \\ 1 & 1 & 1 & 0 & 0 & 1 & 1 & 1 & 0 \\ 1 & 1 & 1 & 0 & 1 & 0 & 0 & 0 & 1 \\ 1 & 1 & 0 & 1 & 0 & 1 & 0 & 0 & 1 \\ 1 & 0 & 1 & 1 & 0 & 0 & 1 & 0 & 1 \\ 0 & 1 & 1 & 1 & 0 & 0 & 0 & 1 & 1 \\ 0 & 0 & 0 & 0 & 1 & 1 & 1 & 1 & 1 \end{pmatrix}$$

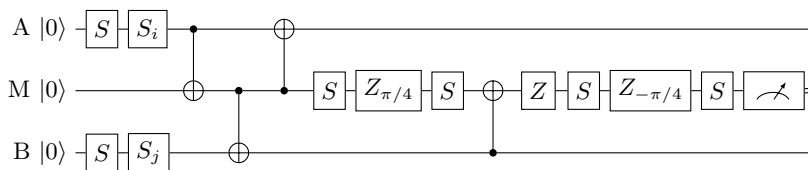
TABLE II. Binary matrices $n \times n$ with the maximal W_n given in Table I.

FIG. 2. The implementation of the test on IBM Quantum.

$n \setminus d$	$2r$	$2c$	$3r$	$3c$	$4rc$
2	1				
3	0.316		2		
4	0	0.111	0.903		3
5	0	0	0.297	0.333	1.874

TABLE III. The calculated fully quantum maxima for the test of the witness quantity W_n for the dimension d , with (r/c) denoting the real/complex case. The empty cell takes the nearest value on the left.

2). The newest devices use Echoed Crossed Resonance (*ECR*) gate, instead of *CNOT* but one can transpile the latter by additional single-qubit gates, see Appendix B.

The parties create the states on the non-planar Viviani curve on the Bloch sphere. For the sake of clarity, let us focus on party *A*. One can use the Bloch sphere representation of prepared states and measurements, using vectors \mathbf{a} to represent the state $A = |\mathbf{a}\rangle\langle\mathbf{a}| = (1 + \mathbf{a} \cdot \boldsymbol{\sigma})/2$, with Pauli matrices $\sigma_{1,2,3}$. The initial state $|0\rangle\langle 0|$ corresponds to the vector $(0, 0, 1)$. The $\pi/2$ rotations by *S* gate and phase shifted rotations S_α allow to obtain the nonplanar parametric Viviani curve on the Bloch sphere. Let us recall that the Viviani curve arises as the intersection of a cylinder tangent to a sphere and embedded inside it, passing through the origin. It gives the prepared state $A_i = |\psi_i\rangle\langle\psi_i|$ with $|\psi_i\rangle = S_i S|0\rangle$ for $S_i \equiv S_{\alpha_i}$. In our specific sequences, the states from Viviani curve $\mathbf{a} = -(\sin \alpha \cos \alpha, \sin^2 \alpha, \cos \alpha)$ for α_k , $k = 1, 2, 3, 4, 5$, correspond to $\pi/4, -\pi/4, 3\pi/4, -3\pi/4, 0$, respectively.

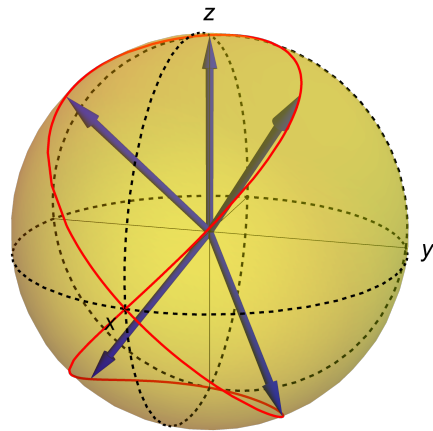


FIG. 3. The Bloch vectors for the sets of preparations used in the work

We swap the state *A* to *M* by a pair of $CNOT_\uparrow CNOT_\downarrow$ on *AM*, with *M* initialized as $|0\rangle$. Now the measurement is operationally determined by the outcome 0 on the qubit *M* while the other ones are ignored. We have implemented so the following measurement operator

$$\mathcal{M} = |00\rangle\langle 00| + (|01\rangle + |10\rangle)(\langle 01| + \langle 10|)/2, \quad (7)$$

by the unitary mapping to the $\mathcal{M}' = |00\rangle\langle 00| + |01\rangle\langle 01|$ in the *MB* space, Indeed, the projection on the final state $\langle 0|$ of *M* results in

$$\langle 0|SZ_{-\pi/4}SZ = \langle \phi|. \quad (8)$$

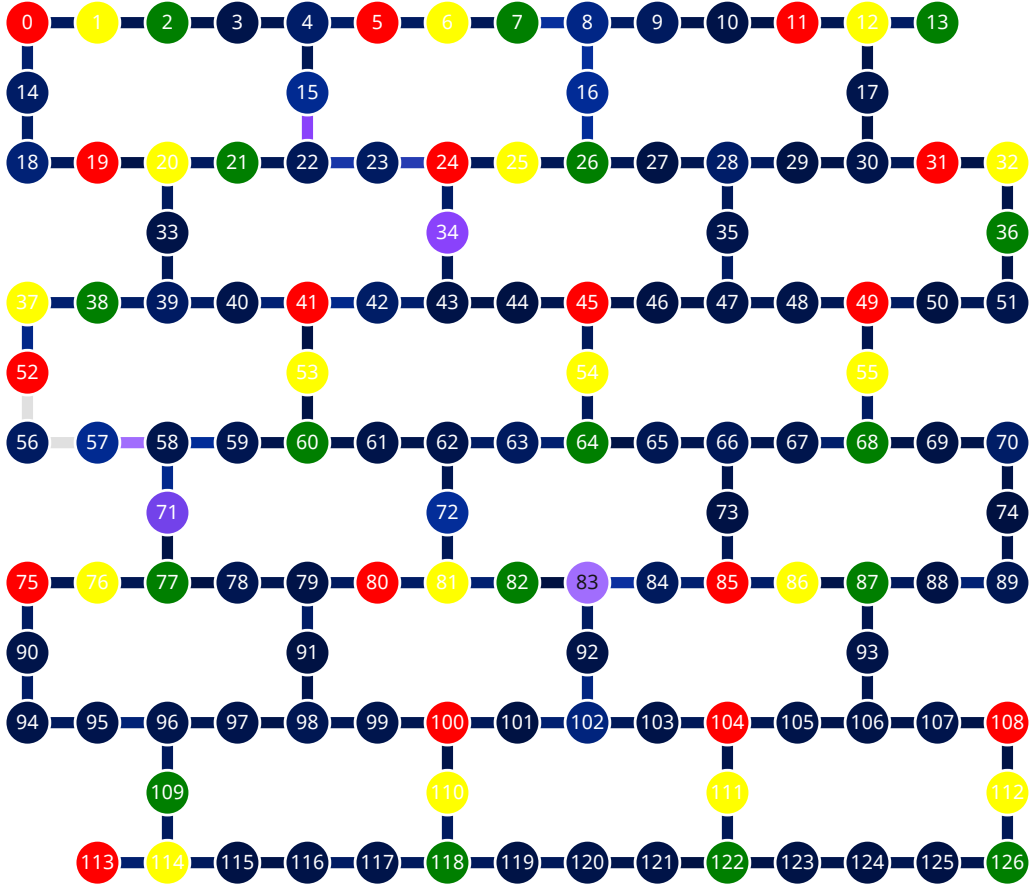


FIG. 4. Topology of the qubit grid of IBM Quantum devices in Eagle generation, *ibm_sherbrooke*, Here the circles represent qubits, bars connections for two-qubit gates. The grid is actually hexagonal. The tested set of qubits are designated: *A* – red, *M* – yellow, *B* – green

Now if the other qubit is in the final state $\langle 0|$ then $\langle \phi 0 | CNOT_{\uparrow} = \langle \phi 0 |$ and

$$\langle \phi | SZ_{\pi/4} S = \langle 0 |, \quad (9)$$

since

$$S^2 = -iX, \quad SZ = ZS^{\dagger}, \quad (10)$$

and again $\langle 00 | CNOT_{\downarrow} = \langle 00 |$. On the other hand if the other qubit is in the state $\langle 1|$ then $\langle \phi 1 | CNOT_{\uparrow} = \langle \phi' 1 |$ with $\langle \phi' | = \langle \phi | X$ and

$$\begin{aligned} \langle \phi' | SZ_{\pi/4} S &= \langle 0 | SZ_{-\pi/4} SZX SZ_{\pi/4} S = \\ \langle 0 | SZ_{-\pi/4} ZX Z_{\pi/4} S &= \langle 0 | X SZ_{\pi/4} Z Z_{\pi/4} S = \\ \langle 1 | SZ_{-} S &= (\langle 0 | + \langle 1 |) / \sqrt{2}, \end{aligned} \quad (11)$$

ignoring global phases, while

$$(\langle 01 | + \langle 11 |) CNOT_{\downarrow} = \langle 01 | + \langle 10 | \quad (12)$$

The probability matrix p_{ij} in this case reads

$$\frac{1}{8} \begin{pmatrix} 5 - \sqrt{8} & 4 - \sqrt{8} & 4 & 5 & 2 - \sqrt{2} \\ 4 - \sqrt{8} & 5 - \sqrt{8} & 5 & 4 & 2 - \sqrt{2} \\ 4 & 5 & 5 + \sqrt{8} & 4 + \sqrt{8} & 2 + \sqrt{2} \\ 5 & 4 & 4 + \sqrt{8} & 5 + \sqrt{8} & 2 + \sqrt{2} \\ 2 - \sqrt{2} & 2 - \sqrt{2} & 2 + \sqrt{2} & 2 + \sqrt{2} & 0 \end{pmatrix}, \quad (13)$$

with its adjugate

$$\frac{1}{2^9} \begin{pmatrix} -1 & +1 & -1 & +1 & 0 \\ +1 & -1 & +1 & -1 & 0 \\ -1 & +1 & -1 & +1 & 0 \\ +1 & -1 & +1 & -1 & 0 \\ 0 & 0 & 0 & 0 & 0 \end{pmatrix}. \quad (14)$$

Each test consists of a certain number of jobs, where each circuit (randomly shuffled) is run a certain number of shots. Since the number of experiments is 25, each one could be repeated to saturate the limit on circuits. The total number of trials is $N = \#jobs \#shots \#repetitions$. Due to calibration changes, every several hours, the probabilities may drift, which can affect the witness being a nonlinear function of probabilities. To take it into account, we have calculated the witness in two ways [21]:

W' , $\Delta W'$ – the witness is obtained from total probabilities of all jobs together; W'' , $\Delta W''$ – is obtained by calculating probabilities and the witness for each job individually, and then averaging it over jobs. It turns out that these values indeed differ but do not change the verdict about dimension. We have run two types of gates scheduling: *as late as possible* (ALAP or L), *as soon as possible* (ASAP or S). They differ by the timing of the gate operations. In the ALAP scheduling, the gates are applied at the very last to avoid premature decoherence of the qubits, which are initially in the ground state $|0\rangle$. In the ASAP scheduling, the gates are applied immediately after the start of the shot or after the previous operation. In the ALAP/ASAP scheduling we have run 60/40 jobs with 4 repetitions and 20000 shots. Out of 17 preselected sets of qubits, shown in Fig. 4, on *ibm_sherbrooke* and one in *ibm_brisbane* most of them passed the test. Only two sets, one in *ibm_sherbrooke* and one in *ibm_brisbane*. The final witness for these cases disagrees with the null hypothesis for $d = 2$ beyond 10 standard deviations see Table IV. However, the *ibm_brisbane* case gives 4 times smaller deviation in the ASAP case. The distribution of witnesses for individual jobs is consistent with the average, Fig. 5. The accuracy of our test is especially clear when looking at the probability matrix, Fig. 6, which naively resembles the theoretical prediction, while the exact calculation of the witness reveals the deviation.

To explain the nonzero value of W by small corrections to probabilities of any origin, i.e. $p \rightarrow p + \delta p$, one can estimate $\delta W = \text{Tr} \mathcal{A} \delta p$ for the adjugate matrix \mathcal{A} . The elements of the adjugate matrix are of the order $\lesssim 10^{-3}$. Since the local leakage to higher excited states is $\lesssim 10^{-6}$ [22] and the fact that the error is squared, i.e. $\delta p_{ij} \sim 10^{-12}$, giving the contribution to the deviation of the determinant $\sim 10^{-15}$, much below the observed values $W \gtrsim 10^{-5}$. The *CNOT/ECR* gates with errors $\sim 10^{-2}$ could affect the determinant only if they are correlated with preparations, which would indicate a complete technical failure. The data and scripts are publicly available [23].

V. CONCLUSIONS

We have demonstrated the extreme usefulness of null tests of the Schmidt number for the bipartite states, which should help in the diagnostics of quantum devices. It is complementary to the violation of a Bell-type inequality while based on similar assumptions. Combining it with no-signaling verification and Bell-type violations in a single test can serve as a powerful quality criterion of multiqubit networks. We stress that our null hypothesis tests remain robust against most common disturbances, as long as they are local, with known mechanisms. Due to the extreme accuracy of the test, we were able to diagnose IBM Quantum devices, far beyond standard technical specifications. The results showed consistency with

the Schmidt number $d = 2$ in the case of independent measurements but the test with many outcomes failed to confirm it. The deviation is significant and exceeds possible common origins due to gate errors. The failure requires an urgent technical explanation. Otherwise, the results may be a signature of an exotic picture, involving e.g. many worlds/copies [24, 25] (N copies of the same system formally boost the dimension from d to d^N). We refrain from giving an exact model, as the collected data are insufficient to draw stronger conclusions.

ACKNOWLEDGMENTS

The results have been created using IBM Quantum. The views expressed are those of the authors and do not reflect the official policy or position of IBM Quantum team. We acknowledge technical support of Tomasz Rybotycki, Tomasz Bialecki, Jakub Tworzydło, Bartłomiej Zglinicki, and Bednorz family.

Appendix A: Quantum maxima of the witness

The following results have been obtained by using a simulated annealing optimization method for the determinant, plus some intuition being guided by the existing symmetry for each case. The ensuing results are later polished by making use of symbolic mathematical packages.

Case $n = 3$, $d = 2$. Real and complex maximum is $(3/4)^4 = 0.31640625$ for $A_i = B_i = |\psi_i\rangle\langle\psi_i|$ with

$$|\psi_j\rangle = \cos(2\pi j/3)|0\rangle + \sin(2\pi j/3)|1\rangle, \quad (\text{A1})$$

for $j = 1, 2, 3$ and rank 3 projection

$$\mathcal{M} = |00\rangle\langle 00| + |11\rangle\langle 11| + (|01\rangle - |10\rangle)(\langle 01| - \langle 10|)/2. \quad (\text{A2})$$

With only two projections, it is lower $1/8 = 0.125$ in the real case with

$$3\mathcal{M} = 3|00\rangle\langle 00| + 3|01\rangle\langle 01| + 3|10\rangle\langle 10| - (|00\rangle + |01\rangle + |10\rangle)(\langle 00| + \langle 01| + \langle 10|), \quad (\text{A3})$$

or $3^6/5^5 = 0.23328$ in the complex case with

$$|\psi_j\rangle = \sqrt{3/5}|0\rangle + \sqrt{2/5}\omega^j|1\rangle,$$

for $\omega = e^{2\pi i/3} = (\sqrt{3}i - 1)/2$, and

$$\mathcal{M} = |00\rangle\langle 00| + (|01\rangle - |10\rangle)(\langle 01| - \langle 10|)/2. \quad (\text{A4})$$

For a single projection the maximum is $3^3/2^8 = 0.10546875$ for both real and complex case

$$|\psi_j\rangle = \cos(2\pi j/3)|0\rangle + \sin(2\pi j/3)|1\rangle \quad (\text{A5})$$

for $j = 1, 2, 3$, and

$$\mathcal{M} = (|01\rangle - |10\rangle)(\langle 01| - \langle 10|)/2. \quad (\text{A6})$$

device	$A - M - B$	W_5^L	ΔW_5^L	$W_5^{L'}$	$\Delta W_5^{L'}$	W_5^S	ΔW_5^S	$W_5^{S'}$	$\Delta W_5^{S'}$	f_{AB}
<i>ibm_brisbane</i>	11-12-13	24.45	0.57	24.44	0.58	5.48	0.50	5.39	0.51	-34
<i>ibm_sherbrooke</i>	108-112-126	18.33	1.07	18.43	1.08	21.23	1.24	21.00	1.25	26

TABLE IV. The values of the witnesses W and W' with their errors ΔW and $\Delta W'$ in units 10^{-6} for the ALAP (L) and ASAP (S) tests on the most faulty qubits A, M, B . We have also shown the difference between frequencies of qubits A and B , $f_{AB} = f_A - f_B$ in units MHz.

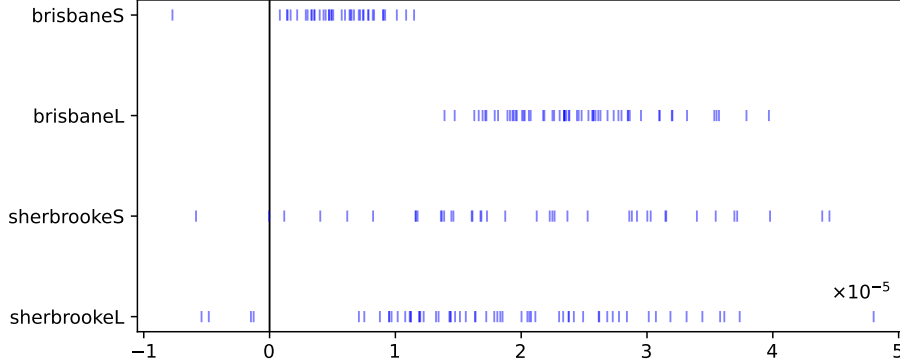


FIG. 5. The individual values of the witness for the most faulty sets in *ibm_brisbane* and *ibm_sherbrooke*, for ALAP/ASAP tests, brisbaneL/S, sherbrookeL/S, respectively.

Case $n = 4$, $d = 2$ complex, we get $W = 1/9$ for

$$\begin{aligned} \sqrt{3}|\psi_j\rangle &= |0\rangle + \omega^j\sqrt{2}|1\rangle, \\ |\psi_4\rangle &= |0\rangle, \end{aligned} \quad (\text{A7})$$

for $j = 1, 2, 3$, and \mathcal{M} of the form (A2).

Case $n = 4$, $d = 3$ real and complex we obtain the tetrahedral configuration

$$\begin{aligned} \sqrt{3}|\psi_1\rangle &= |0\rangle + |1\rangle + |2\rangle, \\ \sqrt{3}|\psi_2\rangle &= |0\rangle + |1\rangle - |2\rangle, \\ \sqrt{3}|\psi_3\rangle &= |0\rangle - |1\rangle + |2\rangle, \\ \sqrt{3}|\psi_4\rangle &= |0\rangle - |1\rangle - |2\rangle, \end{aligned}$$

and rank 5 projection

$$\mathcal{M} = \sum_{i \neq j} (|ij\rangle + |ji\rangle)\langle ij|/2 + \sum_i 2|ii\rangle\langle ii|/3 - \sum_{i \neq j} |ii\rangle\langle jj|/3, \quad (\text{A8})$$

for $i, j = 0, 1, 2$, which gives $-W = 2^8 5^4 / 3^{11} \simeq 0.903204683116282$.

Case $n = 5$, $d = 3$ real. We numerically retrieve 0.2974087137533708 for the preparations

$$\begin{aligned} 2|\psi_1\rangle &= -|0\rangle + \sqrt{3}|1\rangle, \\ 2|\psi_2\rangle &= -|0\rangle - \sqrt{3}|1\rangle, \\ |\psi_3\rangle &= |0\rangle, \\ 2|\psi_4\rangle &= -|0\rangle + \sqrt{3}|2\rangle, \\ 2|\psi_5\rangle &= -|0\rangle - \sqrt{3}|2\rangle, \end{aligned} \quad (\text{A9})$$

and rank 5 projection

$$\mathcal{M} = \sum_{ij} |ij\rangle\langle ij| - \sum_{j=1}^4 |\phi_j\rangle\langle\phi_j|, \quad (\text{A10})$$

for

$$\begin{aligned} |\phi_1\rangle &= |22\rangle, \\ |\phi_2\rangle &= p|10\rangle - q|02\rangle, \\ |\phi_3\rangle &= p|01\rangle - q|20\rangle, \\ |\phi_4\rangle &= x(|12\rangle + |21\rangle) - y|00\rangle, \end{aligned} \quad (\text{A11})$$

giving

$$\begin{aligned} W &= (3^8/2^{10})(pq + xy)^2 \times \\ &(2x^2(x^2 + y^2)^2 - 2p^2q^2(x^2 + y^2) + p^4), \end{aligned} \quad (\text{A12})$$

for $p^2 + q^2 = 1 = x^2 + 2y^2$, optimal for $x^2 = 0.28105400986117085$, $p^2 = 0.8688370017274547$.

Case $n = 5$, $d = 3$ complex. We have to take $A_j = |a_j\rangle\langle a_j|$, $B_j = |b_j\rangle\langle b_j|$, with

$$\begin{aligned} |a_j\rangle &= x|0\rangle + y|1\rangle + z\omega^j|2\rangle, \\ |a_4\rangle &= s|0\rangle + t|1\rangle, |a_5\rangle = |0\rangle \\ |b_j\rangle &= p|0\rangle + q\omega^j|1\rangle + r\omega^{2j}|2\rangle, \\ |b_4\rangle &= |0\rangle, |b_5\rangle = |1\rangle, \end{aligned} \quad (\text{A13})$$

with again $\omega = e^{2\pi/3}$, and rank 5 projection

$$\begin{aligned} \mathcal{M} &= |01\rangle\langle 01| + |02\rangle\langle 02| \\ &+ |12\rangle\langle 12| + |13\rangle\langle 13| + |20\rangle\langle 20| + |21\rangle\langle 21| \\ &+ |\psi_1\rangle\langle\psi_1| - |\psi_2\rangle\langle\psi_2| - |\psi_3\rangle\langle\psi_3|, \end{aligned} \quad (\text{A14})$$

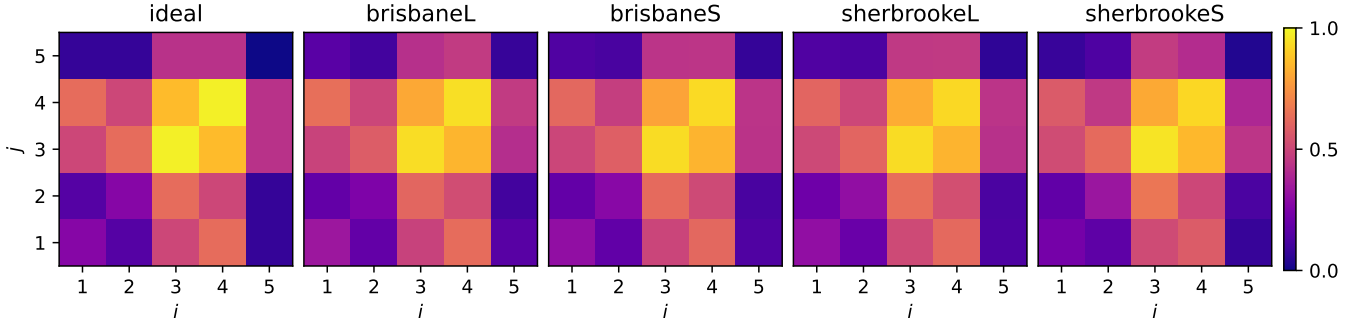


FIG. 6. The probabilities p_{ij} for the most faulty sets in *ibm_brisbane* and *ibm_sherbrooke*, for ALAP/ASAP, tests, brisbaneL/S, sherbrookeL/S, respectively, compared to the ideal prediction.

with

$$\begin{aligned} |\psi_1\rangle &= c|00\rangle + d|10\rangle + e|22\rangle, \\ |\psi_2\rangle &= f|01\rangle + g|11\rangle + h|20\rangle, \\ |\psi_3\rangle &= u|02\rangle + v|12\rangle + w|21\rangle. \end{aligned} \quad (\text{A15})$$

It yields

$$\begin{aligned} W &= 27t(\alpha + 2s\beta)r^2z^2 \times \\ &(\text{pre}(cx + dy) - pqh(fx + gy) - qrw(ux + vy))^2, \end{aligned} \quad (\text{A16})$$

with

$$\begin{aligned} \alpha &= 2xyuv(c^2(1-g^2) - d^2(1-f^2)) + \\ &(2xycd + z^2(1-h^2)) \times \\ &((1-u^2)(1-g^2) - (1-v^2)(1-f^2)) \\ &+ (2xyfg + w^2z^2)(d^2(1-u^2) - c^2(1-v^2)) + \\ &z^2((c^2 - d^2)(1-e^2) + (g^2c^2 - d^2f^2)e^2 + d^2u^2 - c^2v^2), \end{aligned} \quad (\text{A17})$$

and

$$\begin{aligned} \beta &= y^2(cd(g^2 - f^2 + u^2(1-g^2) - v^2(1-f^2)) + \\ &fg(c^2(1-v^2) - d^2(1-u^2)) + \\ &(d^2(1-f^2) - c^2(1-g^2))uv) \\ &+ z^2(uv((1-f^2)(1-h^2) - c^2(1-w^2)) \\ &- cd((1-u^2)(1-w^2) - e^2(1-f^2)) \\ &- fg((1-u^2)(1-h^2) - c^2e^2)), \end{aligned} \quad (\text{A18})$$

with constraints

$$\begin{aligned} x^2 + y^2 + z^2 &= c^2 + d^2 + e^2 = 1, \\ f^2 + g^2 + h^2 &= u^2 + v^2 + w^2 = 1, \\ p^2 + q^2 + r^2 &= s^2 + t^2 = 1. \end{aligned} \quad (\text{A19})$$

The last constraint implies the maximum

$$\begin{aligned} W &= 27(\alpha/2 + \sqrt{\alpha^2/4 + \beta^2})r^2z^2 \times \\ &(\text{pre}(cx + dy) - pqh(fx + gy) - qrw(ux + vy))^2 \times \\ &(\alpha/2 + \sqrt{\alpha^2/4 + \beta^2}) \end{aligned} \quad (\text{A20})$$

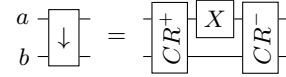


FIG. 7. The notation of the *ECR* gate in the convention $ECR_{\downarrow}(ab)$.

which we calculated at 0.33262772907714405.

Finally, the case $d = 4$, $n = 5$ gives the maximum for a 5-cell (a regular simplex in four-dimensional space) configuration, parameterized e.g. by

$$\begin{aligned} 4|\psi_1\rangle &= \sqrt{5}(|1\rangle + |2\rangle + |3\rangle) - |0\rangle, \\ 4|\psi_2\rangle &= \sqrt{5}(|1\rangle - |2\rangle - |3\rangle) - |0\rangle, \\ 4|\psi_3\rangle &= \sqrt{5}(|2\rangle - |3\rangle - |1\rangle) - |0\rangle, \\ 4|\psi_4\rangle &= \sqrt{5}(|3\rangle - |1\rangle - |2\rangle) - |0\rangle, \\ |\psi_5\rangle &= |0\rangle, \end{aligned} \quad (\text{A21})$$

with rank 11 projection

$$\mathcal{M} = \sum_{ij} |ij\rangle\langle ij| - \sum_k 16|\tilde{k}\rangle\langle\tilde{k}|/15 + 4|e\rangle\langle e|/75 \quad (\text{A22})$$

for $|\tilde{k}\rangle = |\psi_k\psi_k\rangle$ and $|e\rangle = \sum_k |\tilde{k}\rangle$. Here, \mathcal{M} is essentially a projection orthogonal to each $|\tilde{k}\rangle$. It gives the matrix entries

$$p_{ij} = \begin{cases} 55/64 & \text{for } i \neq j, \\ 0 & \text{for } i = j, \end{cases} \quad (\text{A23})$$

with the result

$$W = 4(55/64)^5 = 1.8748803995549678802490234375. \quad (\text{A24})$$

Appendix B: Gates and transpiling at IBM Quantum

We shall use Pauli matrices in the basis $|0\rangle, |1\rangle$,

$$X = \begin{pmatrix} 0 & 1 \\ 1 & 0 \end{pmatrix}, Y = \begin{pmatrix} 0 & -i \\ i & 0 \end{pmatrix}, Z = \begin{pmatrix} 1 & 0 \\ 0 & -1 \end{pmatrix}, I = \begin{pmatrix} 1 & 0 \\ 0 & 1 \end{pmatrix}. \quad (\text{B1})$$

The IBM Quantum devices (*ibm_brisbane*) use transmon qubits [26] with the native single qubit gates are X and

$$X_+ = X_{\pi/2} = (I - iX)/\sqrt{2} = \begin{pmatrix} 1 & -i \\ -i & 1 \end{pmatrix} / \sqrt{2}, \quad (\text{B2})$$

denoting $V_\theta = \exp(-i\theta V/2) = \cos(\theta/2) - iV \sin(\theta/2)$ and $V_\pm = V_{\pm\pi/2}$, whenever V^2 is identity. Note that $Z_\theta = \exp(-i\theta Z/2) = \text{diag}(e^{-i\theta/2}, e^{i\theta/2})$ is a virtual gate adding essentially the phase shift to next gates. [27]

A native two-qubit gate in IBM Quantum is Echoed Cross Resonance (ECR) instead of $CNOT$ [28]. One can transpile the latter by the former, adding single qubit gates. The ECR gate acts on the states $|ab\rangle$ as (Fig. 7)

$$ECR_\downarrow = ((XI) - (YX))/\sqrt{2} = CR^-(XI)CR^+ = \begin{pmatrix} 0 & X_- \\ X_+ & 0 \end{pmatrix} = \begin{pmatrix} 0 & 0 & 1 & i \\ 0 & 0 & i & 1 \\ 1 & -i & 0 & 0 \\ -i & 1 & 0 & 0 \end{pmatrix} / \sqrt{2}, \quad (\text{B3})$$

in the basis $|00\rangle, |01\rangle, |10\rangle, |11\rangle$, with Crossed Resonance gates

$$CR^\pm = (ZX)_{\pm\pi/4}. \quad (\text{B4})$$

The gate is its inverse, i.e. $ECR_\downarrow ECR_\downarrow = (II)$. It can be reversed, i.e., for $a \leftrightarrow b$, we have (Fig. 8)

$$ECR_\uparrow = ((IX) - (XY))/\sqrt{2} = (HH)ECR_\downarrow(Y_+Y_-), \quad (\text{B5})$$

and Hadamard gate

$$H = (Z + X)/\sqrt{2} = Z_+X_+Z_+ = \begin{pmatrix} 1 & 1 \\ 1 & -1 \end{pmatrix} / \sqrt{2} \quad (\text{B6})$$

and $Z_\pm X_+ Z_\mp = Y_\pm$, with $Y_+ = HZ$ and $Y_- = ZH$. The $CNOT$ gate can be expressed by ECR (Fig. 9)

$$CNOT_\downarrow = ((II) + (ZI) + (IX) - (ZX))/2 = \begin{pmatrix} I & 0 \\ 0 & X \end{pmatrix} = \begin{pmatrix} 1 & 0 & 0 & 0 \\ 0 & 1 & 0 & 0 \\ 0 & 0 & 0 & 1 \\ 0 & 0 & 1 & 0 \end{pmatrix} = (Z_+I)ECR_\downarrow(XX_+), \quad (\text{B7})$$

while its reverse reads (Fig. 10)

$$CNOT_\uparrow = ((II) + (IZ) + (XI) - (XZ))/2 = \begin{pmatrix} 1 & 0 & 0 & 0 \\ 0 & 0 & 0 & 1 \\ 0 & 0 & 1 & 0 \\ 0 & 1 & 0 & 0 \end{pmatrix} = (HH)CNOT_\downarrow(HH) = (HH)ECR_\downarrow(X_+X_+)(Z_-H). \quad (\text{B8})$$

-
- [1] A. Einstein, B. Podolsky, N. Rosen, *Can Quantum-Mechanical Description of Physical Reality Be Considered Complete?* Phys. Rev. **47**, 777 (1935).
- [2] J.S. Bell, *On the Einstein Podolsky Rosen paradox*, Physics (Long Island City, N.Y.) **1**, 195 (1964).
- [3] J.F. Clauser, M.A. Horne, A. Shimony and R.A. Holt, *Proposed Experiment to Test Local Hidden-Variable Theories*, Phys. Rev. Lett. **23**, 880(1969).
- [4] J.F. Clauser, M.A. Horne, *Experimental consequences of objective local theories*, Phys. Rev. D **10**, 526 (1974)
- [5] P.H. Eberhard, *Background level and counter efficiencies required for a loophole-free Einstein-Podolsky-Rosen experiment*, Phys. Rev. A **47**, R747 (1993).
- [6] Y. Suzuki, S. Endo, K. Fujii, and Y. Tokunaga, *Quantum Error Mitigation as a Universal Error Reduction Technique: Applications from the NISQ to the Fault-Tolerant Quantum Computing Eras*, Phys. Rev. X **Quantum 3**, 010345 (2022).
- [7] R. Takagi, S. Endo, S. Minagawa, and M. Gu, *Fundamental limits of quantum error mitigation*, npj Quantum Inf. **8**: 114 (2022).
- [8] Z. Cai et al, *Quantum Error Mitigation*, Rev. Mod Phys. **95**, 045005 (2023)
- [9] R. Gallego, N. Brunner, C. Hadley, and A. Acin, *Device-Independent Tests of Classical and Quantum Dimensions*, Phys. Rev. Lett. **105**, 230501 (2010).

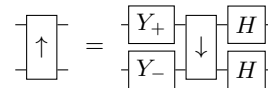


FIG. 8. The ECR_\uparrow gate expressed by ECR_\downarrow

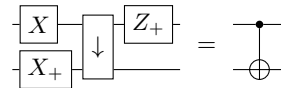


FIG. 9. The $CNOT_\downarrow$ gate expressed by ECR_\downarrow .

- [10] N. Brunner, M. Navascues, and T. Vertesi, *Dimension Witnesses and Quantum State Discrimination* Phys. Rev. Lett. **110**, 150501 (2013).
- [11] J. Bowles, M. T. Quintino, and N. Brunner, *Certifying the Dimension of Classical and Quantum Systems in a Prepare-and-Measure Scenario with Independent Devices*, Phys. Rev. Lett. **112**, 140407 (2014)
- [12] X. Chen K. Redeker, R. Garthoff, W. Rosenfeld, J. Wrachtrup, and I. Gerhardt, *Certified randomness from remote state preparation dimension witness*, Phys. Rev. A **103**, 042211 (2021)
- [13] J. Batle, A Bednorz, Optimal classical and quantum

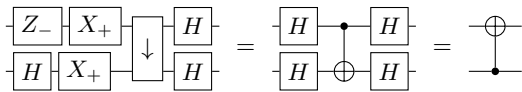


FIG. 10. The $CNOT_{\uparrow}$ gate expressed by ECR_{\downarrow} .

real and complex dimension witness, Phys. Rev. A 105, 042433 (2022)

- [14] T. Bialecki, T. Rybotycki, J. Batle, J. Tworzydło, Adam Bednorz, Precise certification of a qubit space, EPJ Quantum Technol. 11, 21 (2024)
- [15] T. Rybotycki, T. Bialecki, J. Batle, A. Bednorz, Device-independent dimension leakage null test on qubits at low operational cost, Adv. Quantum Technol., 2400264 (2024)
- [16] B. M. Terhal and P. Horodecki, *Schmidt number for density matrices*, Phys. Rev. A 61, 040301(R) (2000).
- [17] A. Sanpera, D. Bruss, and M. Lewenstein, *Schmidt-number witnesses and bound entanglement*, Phys. Rev. A 63, 050301(R) (2001).
- [18] J. Batle, T. Bialecki, T. Rybotycki, J. Tworzydło, A. Bednorz Quantum null-hypothesis device-independent Schmidt rank witness, EPJ Quantum Technology 11, 62 (2024).
- [19] T. P. Le, C. Meroni, B. Sturmfels, R. F. Werner, and T. Ziegler, *Quantum Correlations in the Minimal Scenario*, Quantum 7, 947 (2023).
- [20] M. Nielsen, I. Chuang, Quantum Computation and Quantum Information, Cambridge University Press, 2010.
- [21] T. Bialecki, T. Rybotycki, J. Batle, J. Tworzydło, A. Bednorz, *Precise certification of a qubit space*, EPJ Quantum Technol. 11, 21 (2024)
- [22] T. Rybotycki, T. Bialecki, J. Batle, Adam Bednorz, Advanced Quantum Technologies, 2400264 (2024)
- [23] European Organization For Nuclear Research and Open AIRE, Zenodo, CERN, 2021, <https://doi.org/10.5281/zenodo.14273348>
- [24] R. Plaga, Found. Phys. **27**, 559 (1997)
- [25] A. Bednorz, Annalen der Physik, 201800002 (2018)
- [26] J. Koch, T. M. Yu, J. Gambetta, A. A. Houck, D. I. Schuster, J. Majer, Alexandre Blais, M. H. Devoret, S. M. Girvin, R. J. Schoelkopf, Phys. Rev. A 76, 042319 (2007)
- [27] David C. McKay, Christopher J. Wood, Sarah Sheldon, Jerry M. Chow, Jay M. Gambetta Phys. Rev. A 96, 022330 (2017)
- [28] M. Malekakhlagh, E. Magesan, and D. C. McKay, Phys. Rev. A, 102, 042605 (2020).